HHS Public Access

Author manuscript

Mov Disord. Author manuscript; available in PMC 2016 August 01.

Published in final edited form as:

Mov Disord. 2015 August ; 30(9): 1248–1258. doi:10.1002/mds.26294.

Distinct patterns of brain activity in progressive supranuclear palsy and Parkinson's disease

Roxana G. Burciu, PhD[1], **Edward Ofori, PhD**[1], **Priyank Shukla, PhD**[1], **Peggy J. Planetta, PhD**[1], **Amy F. Snyder, BSc**[1], **Hong Li, PhD**[2], **Chris J. Hass, PhD**[1,6], **Michael S. Okun, MD**[3,4,6], **Nikolaus R. McFarland, MD, PhD**[3,6], and **David E. Vaillancourt, PhD**[1,5,6]

[1]Department of Applied Physiology and Kinesiology, University of Florida, Gainesville, FL, 32611, USA

[2]Department of Preventive Medicine, Rush University Medical Center, Chicago, IL, 60612

[3]Department of Neurology, University of Florida, Gainesville, FL, 32610, USA

[4]Department of Neurosurgery, University of Florida, Gainesville, FL, 32610, USA

[5]Department of Biomedical Engineering, University of Florida, Gainesville, FL, 32611, USA

[6]Center for Movement Disorders and Neurorestoration, University of Florida, Gainesville, FL, 32607, USA

Abstract

Background—The basal ganglia-thalamo-cortical and cerebello-thalamo-cortical circuits are important for motor control. As yet, it is not clear whether their functioning is affected in a similar or different way by progressive supranuclear palsy (PSP) and Parkinson's disease (PD).

Methods—A functional MRI force production paradigm and voxel-based morphometry were used to assess differences in brain activity and macrostructural volumes between PSP, PD, and healthy age-matched controls.

Results—We found that PSP and PD share reduced functional activity of the basal ganglia and cortical motor areas, but this is more pronounced in PSP than in PD. In PSP the frontal regions are underactive, whereas the posterior parietal and occipital regions are overactive as compared to controls and PD. Furthermore, lobules I-IV, V, and VI of the cerebellum are hypoactive in PSP and PD, while Crus I and lobule IX are hyperactive in PSP only. Reductions in gray and white matter volume are specific to PSP. Finally, the functional status of the caudate as well as the volume of the superior frontal gyrus predict clinical gait and posture measures in PSP.

Conclusions—PSP and PD share hypoactivity of the basal ganglia, motor cortex, and anterior cerebellum. PSP patients also display a unique pattern, such that anterior regions of the cortex are hypoactive and posterior regions of the cortex and cerebellum are hyperactive. Together, these findings suggest that specific structures within the basal ganglia, cortex, and cerebellum are affected differently in PSP relative to PD.

Corresponding author: David E. Vaillancourt, PhD, Department of Applied Physiology and Kinesiology, University of Florida, PO Box 118205, (e) vcourt@ufl.edu, (o) +1 352 294 1770, (f) +1 352 392 526.

Keywords

force; functional MRI; progressive supranuclear palsy; Parkinson's disease; motor circuits

Introduction

Progressive supranuclear palsy (PSP) is a tauopathy characterized by neurofibrillary tangles in several cortical and subcortical brain structures (1,2). Patients present with progressive parkinsonism associated with early gait disturbances, frequent falls, vertical gaze palsy, speech difficulty, and cognitive dysfunction (3–5). Although there are accepted clinical criteria for PSP, the diagnosis is not always straightforward, in particular early in the course of the disease when parkinsonian symptoms are sometimes mistaken for idiopathic Parkinson's disease (PD) (4,6). In general, PSP tends to progress more rapidly than PD (4,7,8).

To date, functional magnetic resonance imaging (fMRI) has expanded our understanding of of the functioning of the basal ganglia-thalamo-cortical and cerebello-thalamo-cortical circuits in PD. Specifically, PD is associated with functional changes within all the basal ganglia nuclei, sensorimotor cortex, and cerebellum (9–15). Whether functional activity of the basal ganglia, cortical motor areas or cerebellum in PSP is characterized by changes similar to those observed in PD is not yet clear. More is known about brain morphology rather than brain function in PSP, with degeneration of the midbrain and superior cerebellar peduncles being the most common neuroradiological and neuropathological features (16,17). Least known, yet equally important, is how functional and structural brain differences between these two diseases relate to gait and posture, motor behaviors known to be affected earlier in PSP, and later in PD (4,18,19).

Here, we investigated how motor-related brain activity and macrostructural volumes differ between PSP and PD. Task-based fMRI consisted of a force generation task that has been shown to elicit robust and reproducible results in PD (9–13). For quantifying differences in macrostructural volumes we used voxel-based morphometry (VBM). Since PSP shares parkinsonian features with PD, we hypothesized that both diseases will present with an underactive basal ganglia and cortical motor areas during force production. Given the well-documented atrophy of the superior cerebellar peduncle in PSP, we expected that the cerebellum of these patients will be extensively driven, playing a potential compensatory role. Finally, we sought to determine how functional and structural brain differences between the two patient groups relate to clinical measures of gait and posture. We tested the hypothesis that brain regions involved in higher-order aspects of motor control would provide the best prediction of clinical measures of gait and posture.

Methods

Participants

Sixty individuals participated in this study: 20 PSP, 20 PD, and 20 healthy control individuals (Table 1). The experiment was approved by the Institutional Review Board. All

participants provided informed consent. PSP and PD patients were diagnosed and referred by a fellowship-trained movement disorders specialist at the University of Florida. The degree of their motor impairment was evaluated using the motor section of the MDS-UPDRS (MDS-UPDRS-III) (20). An additional gait and posture composite score was calculated based on items 9-13 of the MDS-UPDRS-III. Participants also completed the Montreal Cognitive Assessment (MoCA) (21). The three groups did not statistically differ for age and gender, and the two patient groups were further matched on symptom severity based on the total MDS-UPDRS-III score. Patients were tested after overnight withdrawal from dopaminergic medication, ca. 12-14 hours after the last dose. Eighteen PD patients presented with a tremor dominant (TD) phenotype, whereas the remaining two had a postural instability/gait difficulty (PIGD) phenotype. The PSP cohort included both the PSP-Parkinsonism and PSP-Richardson subtypes. Additional details on the Hoehn and Yahr stage and disease duration are provided in Table 1. Of note, any interpretation of the current PSP results with respect to disease duration should be made with caution, because disease duration reflects time since diagnosis and not symptom onset. Establishing an accurate clinical diagnosis in PSP takes more time in general, making the estimation of disease duration potentially unreliable.

Apparatus

Grip force control was measured using a custom-designed MRI-compatible fiber optic transducer with a resolution of 0.025 N (Neuroimaging Solutions, Gainesville, FL). Force data were sampled at 125 Hz by a sm130 Fiber Optic Interrogator (Micron Optics, Atlanta, GA) and recorded using LabVIEW (National Instruments, Austin, TX).

Force generation task

We used a well-established force control paradigm (9,10,12,13). Patients produced force with their more affected hand. Controls used either the left or right hand (Table 1). Prior to entering the MRI scanner, all participants were trained on the task and had their maximum pinch grip force (maximum voluntary contraction, MVC) measured.

The fMRI session consisted of a block-design, alternating 30-s force and 12.5-s rest blocks. This sequence was repeated four times. Instructions were presented on an LCD monitor that participants could see through a mirror mounted on the head coil. Two bars were constantly displayed on a black background: a white/stationary target bar, and a colored force bar. Participants were required to move the force bar (by pushing on the force sensor) on top of the target bar. A green force bar instructed participants to generate and maintain force for 2s, and a red force bar instructed the subject to release force for 1s (Fig. 1A). The task was administered under two conditions: a feedback condition where participants could observe the force bar moving across the screen according to the force they applied, and a no-feedback condition where participants could still see the two bars and the change in color that instructed them to push or release, but could not see the force bar moving. In total, there were two feedback and two no-feedback blocks. Target force levels were set at 15% of their MVC.

Force data analysis

Force output was filtered using a 10th order Butterworth filter with a cutoff frequency of 15 Hz. Custom algorithms in MATLAB (The MathWorks, Inc., Natick, MA) were used to calculate the mean force produced across the 30-s force blocks (Fig. 1B). A repeated measures ANOVA with group (PSP, PD, controls) as a between-subjects factor and condition (feedback, no feedback) as a within-subjects factor was applied to mean force. Alpha was set at $p < 0.05$. All statistical analysis was performed using IBM SPSS Statistics 22 (SPSS Inc., Chicago, IL, USA).

Clinical data analysis

Pearson's chi-squared test was applied to categorical data (Table 1). Differences between groups in age, MVC, MDS-UPDRS-III, gait and posture composite MDS-UPDRS-III score, and MoCA were assessed using Kruskal-Wallis H tests. Significant effects were followed up with post-hoc Mann-Whitney U tests. Alpha was set at $p < 0.05$. Corrections for multiple comparisons were applied at a false discovery rate (FDR) of $p < 0.05$ using the Benjamini-Hochberg-Yekutieli method available at http://www.mathworks.com/matlabcentral/fileexchange/27418-benjamini-hochbergyekutieli-procedure-for-controlling-false-discovery-rate/content/fdr_bh.m.

MRI data acquisition

MRI was performed on a 3-T system (Achieva, Philips Medical Systems) equipped with a 32-channel SENSE head coil. Functional images were obtained using a T_2*-weighted, single shot, echo-planar pulse sequence with the following parameters: repetition time = 2500 ms, echo time = 30 ms, flip angle = 80°, field of view = 240 mm^2, acquisition matrix = 80 × 80, voxel size = 3 mm isotropic with no gap between slices (n = 46). The structural imaging protocol consisted of a 3D T_1-weighted sequence: repetition time = 8.2 ms, echo time = 3.7 ms, flip angle = 8°, field of view = 240 mm^2, acquisition matrix = 240 × 240, voxel size = 1 mm isotropic with no gap between slices (n = 170).

MRI data analysis

MRI data analysis was carried out using the Analysis of Functional NeuroImages software package (AFNI) for functional data and Statistical Parametric Mapping (SPM8) in combination with the VBM8 toolbox for structural data. Since the hand used to produce force was not consistent across participants, prior to performing any further preprocessing, functional and structural MRI data of those participants who performed the task with their left hand were flipped along the midline.

Data analysis steps were consistent with those used in our previous studies (9,10,12,13). For each MRI modality, we performed a standard whole-brain analysis as well as a cerebellum-optimized analysis (SUIT, (22,23). Preprocessed fMRI scans were analyzed within the framework of the general linear model, using the six head motion parameters calculated during preprocessing as regressors of no interest. 2 x 2 mixed-effects ANOVA with group (controls vs. PD, controls vs. PSP, and PD vs. PSP) and condition (feedback vs. no-feedback) were applied. Functional data were corrected for Type I error using a Monte Carlo

simulation. The significance level of the contrasts of interest was set at $p < 0.005$, with a minimum cluster size of 324 mm^3, the equivalent of a $p < 0.05$ corrected using the family-wise error rate (FWER). The dependent variables in our VBM analysis were modulated gray (GM) and white (WM) matter segmentations. Independent-samples *t*-tests were used to compare brain morphology between the groups (controls vs. PD, controls vs. PSP, PD vs. PSP). The significance level of all structural contrasts was set at $p < 0.05$, corrected for multiple comparisons using FWER.

Finally, significant fMRI and VBM clusters were anatomically labeled using the Human Motor Area Template (HMAT, (24)), Basal Ganglia Human Area Template (BGHAT, (25)), Automated Anatomical Labeling (AAL; (26)), and probabilistic MRI Atlas of the Human Cerebellum (23).

MRI predictors of gait and posture were tested in a multiple regression analysis with backward stepwise selection. First, we computed percent signal change (PSC) from the functional data in a way consistent with previous work (9, 11). A mean PSC was calculated for each region of interest (ROI) resulting from the PD vs. PSP comparison, based on 10 TRs (i.e., 22.5s) corresponding to the middle section of the force task (an average of the four force blocks). The PSC values corresponding to the functional ROIs were input in the regression model as predictors, while the gait and posture score from MDS-UPDRS-III was treated as a dependent variable. A similar regression analysis was performed for the structural data. The clusters that differed between PD and PSP were used as masks to extract volumetric information that was input in the regression model as predictor while keeping the gait and posture score as the dependent variable. Regression analyses were performed across PD and PSP, as well as separately for each group.

Results

Clinical data

Gender, handedness, hand tested, age, and MVC did not differ between the three groups, and no differences were found in MDS-UPDRS-III between PD and PSP (p_{FDR} values > 0.05). Kruskal-Wallis H tests showed that the gait and posture composite MDS-UPDRS-III score and MoCA differed across the three groups (p_{FDR} values < 0.05) (Table 1). Post-hoc Mann-Whitney U tests revealed that gait and posture and MoCA were significantly reduced in PSP as compared to PD and controls (p_{FDR} values < 0.05). Gait and posture was also impaired in PD relative to controls ($p_{FDR} = 0.001$), but the MoCA was not ($p_{FDR} = 0.056$).

Mean force over 30-s blocks

Figure 1B illustrates force output of one healthy control, one PD patient and one PSP patient during a feedback block. There was a significant condition effect on mean force expressed in percentage of MVC ($F_{1, 57} = 25.90$, $p_{FDR} < 0.001$), with greater force produced during no-feedback [controls = 10.8 (4.6), PD = 8.3 (3.0), PSP = 15.9 (19.3)] vs. feedback [controls = 7.9 (1.2), PD = 7.3 (1.7), PSP = 11.9 (13.9)]. There was no group effect or group by condition interaction (*p* values > 0.05). Similar results were found when examining differences in mean force expressed in Newtons, where a condition effect ($F_{1, 57} = 15.66$, *p*

$_{FDR}$ < 0.001) indicated greater force during no-feedback [controls = 7.4 (3.7), PD = 5.6 (2.6), PSP = 7.01 (4.2)] than feedback [controls = 5.4 (1.7), PD = 4.9 (1.6), PSP = 5.1 (2.7)]. There was no group effect or group by condition interaction on mean force in Newtons (p_{FDR} values > 0.05).

fMRI data

The effect of feedback greater than no-feedback within each ANOVA model was expressed in bilateral BOLD activity in the primary and associative visual cortices, premotor and posterior parietal cortices, as well as midline structures of the cerebellum, consistent with previous studies (27–29). As the group by condition interaction was not significant, and in order to increase statistical power, we report changes in the BOLD signal averaged across feedback and no-feedback. Importantly, the within-group analyses evidenced significant activity for each group in brain areas that are typically involved in motor control (e.g. primary and secondary cortical motor area, basal ganglia, cerebellum; see Supplementary Figure 1), suggesting that patients just like controls performed the task and engaged force-related brain networks.

As shown in Figure 2A, PD and PSP patients had a bilateral reduction in BOLD signal compared with controls throughout the basal ganglia and within cortical motor and premotor regions (Table 2). Although the basal ganglia was hypoactive in both patient groups compared with controls, PSP patients had a significantly more reduced functional activity of the contralateral caudate and ipsilateral putamen compared with PD. Also, PSP had reduced BOLD signal in the lateral portion of the contralateral PMv/M1 compared with PD. The SMA (bilaterally) was hypoactive in PSP compared with controls, whereas the contralateral SMA was hypoactive in PSP compared with PD (Figure 2A, Table 2). Other regions of reduced functional activity in PSP compared with both controls and PD included the frontal and temporal cortices (bilaterally), and ipsilateral thalamus. Compared with PD, PSP also had reduced BOLD activity in the contralateral anterior cingulate cortex, and contralateral inferior parietal lobule. PSP also had an increased BOLD signal compared with controls and PD in the parietal-occipital cortex: lingual and calcarine gyri, cuneus and precuneus, and superior parietal lobule.

BOLD signal in lobules I-IV, V, and VI of the cerebellum was reduced in both PD and PSP compared with controls (Figure 2A, Table 2). Additional hypoactivity in PD was observed in the posterior vermis. A medial cluster spanning the posterior vermis VI and vermis VIIIa/b, and extending into lobule IX (bilaterally) and Crus I/II (contralateral) was hyperactive in PSP compared with PD (Figure 2A). Finally, ipsilateral lobule IX and contralateral Crus I were found to be hyperactive in PSP compared with controls. Panel B in Figure 2 shows the percent signal change during the force task for the ipsilateral SMA, contralateral caudate, ipsilateral superior parietal lobule, and posterior medial cerebellum.

A multiple regression using the backward elimination approach was run in order to determine the functional activity (i.e., percent signal change) of which brain region best predicts gait and posture across PSP and PD, but also separately for each group. For this analysis, all regions that differed between PSP and PD were included in the regression analysis as explanatory variables (n = 14, Table 2), whereas the gait and posture composite

score from MDS-UPDRS-III was set as the dependent variable. A significant model was identified with the percent signal change from the contralateral caudate predicting gait and posture across PSP and PD ($F_{1,39} = 9.44$, $p_{FDR} = 0.004$, $R^2 = 0.199$). Specifically, the lower the functional activity of the caudate, the greater the gait and posture impairment. When performing the regression analysis separate for PSP and PD, the caudate was the only region to predict gait and posture in PSP ($F_{3,19} = 3.34$, $p_{FDR} = 0.046$, $R^2 = 0.385$). None of the regions input in the regression analysis predicted gait and posture in PD (p_{FDR} *values* > 0.05).

VBM data

No significant differences in local GM or WM volume were identified between PD and controls. Compared with controls, PSP patients had reduced GM volume of the contralateral PMd, PMv, putamen, and ipsilateral superior frontal and temporal gyri, and reduced WM volume of the ventral tegmental area (VTA) and ipsilateral superior cerebellar peduncle (SCP) (Figure 3A, Supplementary Table 1). PSP patients had less GM volume than PD in the ipsilateral superior frontal gyrus, and less WM volume in the VTA, and ipsilateral SCP (Figure 3A). Figure 3B depicts the volume of the regions found to differ significantly between PD and PSP (Supplementary Table 1), for each of the three groups. Finally, a multiple regression using backward elimination revealed that the model including the volume of the ipsilateral superior frontal gyrus predicted gait and posture across PSP and PD ($F_{1,39} = 20.97$, $p_{FDR} < 0.001$; $R^2 = 0.356$). The same result was found separately in PSP ($F_{1,19} = 6.44$, $p_{FDR} < 0.021$; $R^2 = 0.264$), but not in PD (p_{FDR} *values* > 0.05). That is, the more reduced the volume of the superior frontal gyrus, the more impaired the gait and posture in PSP.

Discussion

The current findings demonstrate different patterns of motor-related brain activity across the basal ganglia-thalamo-cortical and cerebello-thalamo-cortical circuits in PSP compared with PD. The results show that PSP and PD share reduced basal ganglia and motor and premotor cortical activity, but this is more pronounced in PSP than in PD. In PSP the frontal regions of the brain are less active, whereas the posterior parietal and occipital cortices are hyperactive relative to controls and PD. Furthermore, lobules I-IV, V, and VI of the cerebellum are hypoactive in PSP and PD, while Crus I and lobule IX are hyperactive in PSP only. As for structural brain differences, PSP have extensive gray and white matter atrophy as compared to PD patients who presented with no volumetric abnormalities. Finally, reduced functional activity of the caudate and reduced volume of superior frontal gyrus predict clinical gait and posture impairment across PSP and PD.

Functional MRI analysis revealed widespread hypoactivity within the basal ganglia circuit and sensorimotor cortex in both PSP and PD as compared with controls. A key finding was that functional activity of the caudate and PMv (extending into M1) contralateral to the tested hand, and the ipsilateral putamen were further decreased in PSP compared with PD. Precision-grip paradigms are known to engage multiple brain networks (30,31), as evidence in Supplementary Figure 1. Given that both sides of the basal ganglia are involved in the

precision task, it follows that PSP patients could have deficits on both sides of the basal ganglia. It is possible that both corticostriatal and interhemispheric interactions are altered in PSP as compared to PD.

The basal ganglia results parallel that of Brooks and colleagues (32) who demonstrated lower caudate [^{18}F]DOPA uptake in PSP relative to PD, collectively suggesting greater dopamine denervation within the basal ganglia of PSP patients, but also dysfunction within the cognitive circuits of the basal ganglia (33,34). We also provide new evidence that caudate activity was a significant predictor of clinical measures of gait and posture in PSP, but not in PD. Alterations of the striatal dopamine and cerebral glucose metabolism have been previously reported in PD patients with freezing of gait, who showed a significantly reduced uptake of ^{18}[F]-6-fluoro-levodopa (FDOPA) and ^{18}[F]-fluordesoxyglucose (FDG) in the caudate nucleus (35). Furthermore, evidence for the involvement of the caudate in maintaining posture and gait comes from elderly, where shape abnormalities of the caudate nucleus correlated with poorer gait and balance (36). With the caudate nucleus being interconnected with the dorso- and ventro-lateral prefrontal areas (37,38), gait and postural control may be related to impaired cognitive control of complex movement sequences. The significant relationship between the volume of higher-order structures such as the superior frontal gyrus and gait and posture appears to favor the hypothesis of dysfunction at the interface of motor and cognitive processes.

It is important to note that although the PD patients tested in this study were predominantly tremor-dominant. The PD patients still had gait and posture impairments, but to a lesser degree than PSP. This could potentially explain the lack of a significant correlation between caudate activity and gait and posture in this cohort. Although speculative, it may well be that gait and posture in PD will deteriorate with disease progression and result in functional brain changes similar to those observed in PSP. Given that we used clinical ratings of gait and posture pertaining to the MDS-UPDRS-III, it would be useful in the future to examine the association between functional brain differences in PSP and PD and more specific and quantifiable parameters (e.g. stride length, swing time, or variability), and how these measures change with time.

Consistent with prior studies (9,10,39), the BOLD signal in the SMA was reduced in PD compared with controls. Similar to the basal ganglia results, the SMA activity was further reduced in PSP as compared to PD. The basal ganglia and SMA are critical for both self-initiated and externally triggered movements (40), and these results point to a greater dysfunction within the basal ganglia-SMA circuit in PSP than in PD. Another interesting finding in PSP is a combination of hypoactivity of the prefrontal cortex with hyperactivity of the posterior parietal and occipital cortices, relative to both PD and controls. Hypoactivity of the anterior regions in PSP may be related to impairment of the frontal-subcortical circuits known to mediate aspects of cognition (41). Hyperactivity of the posterior parietal cortex in PSP as compared to PD and controls may indicate a pathological state. An imaging study of power grip in healthy participants revealed a stronger parietal activity at 10% MVC as compared to 20% MCV, and more variability was observed at the individual level for lower force ranges (42). In the same study, activity of the posterior cerebellum seemed to mirror that of the parietal cortex, with a slightly higher activity at lower forces than higher forces.

Force variability was recently linked in healthy individuals to an increased electrical activity of the parietal cortex during a precision grip task (43). Therefore, it cannot be excluded that the hyperactivity of the parietal cortex in PSP is related to the higher variability of force observed in this group. Another potential hypothesis is the compensatory one. Importantly, the posterior parietal cortex represents a node in the fronto-parietal network, and has been linked not only to sensory integration but also attentional control of task goals (44,45). Therefore, it is possible that the parietal node increases its processing demands and becomes more engaged in aspects of cognitive control of movement which is typically associated with the frontal brain structures shown to be underactive in this population.

With respect to the cerebellum, we confirmed the hypothesis of increased functional activity in PSP as compared to PD and controls. However, we also found evidence for reduced cerebellar activity in PSP relative to controls. Lobules I-IV, V, and VI are known to be involved in the control of voluntary hand movements (46–48), and interestingly, lobules I-V are underactive in essential tremor patients during a similar task (12). Here, functional activity of Crus I, lobule IX, vermis VI, and vermis VIIIa/b was increased in PSP compared with PD. The hypoactivity of the anterior structures of the cerebellum in PD and PSP may arise from a similar mechanism. Given the known connections of the anterior motor structures to the primary motor cortex (49–51), it could be that lobules V-VI are receiving diminished input from the supratentorial structures. From previous studies mapping the connections of the cerebellum to the cerebrum (49,51–53), there is a functional gradient within the cerebellum such that caudal cerebellar regions are connected to regions related to higher levels of motor control. Also, a review of fMRI studies (48) proposes a functional somatotopy of the cerebellum, with posterior and inferior regions of the cerebellum involved in more complex motor tasks. Since we observed that caudate BOLD activity was reduced in PSP and was a significant predictor of gait and posture, it could be that the posterior and inferior regions of the cerebellum are attempting to compensate for this deficit.

With respect to brain structure, PSP patients had significant gray matter volume reduction in the premotor cortex, putamen, superior frontal gyrus, results that is consistent with previously published work (54–57). In addition, atrophy of ventral tegmental area and superior cerebellar peduncle was detected, reinforcing previous findings (58–60). In particular, atrophy of white matter tracts in PSP relative to PD and controls suggests disruption of the dentate-thalamo-cortical pathways. As for PD, no gray or white matter volumetric abnormalities were found. These results confirm some of the previous findings (61), and suggest that gross morphological (volumetric) changes in PD could emerge later in the disease course when patients present with additional non-motor symptoms (62,63).

Finally, no group differences were found in the mean force data. Of note, the analysis performed in this study consisted of assessing the mean force produced during the entire force blocks. Prior work by our group (64) has described in greater detail characteristics of the individual force pulses in PSP and PD patients relative to controls. For instance, it has been shown that rate of contraction and relaxation is slower in both PD and PSP as compared to controls, which is consistent with both groups experiencing bradykinesia.

In summary, both patient groups share an underactive basal ganglia, motor cortex, and anterior cerebellum. In addition, PSP patients display a unique pattern, such that the more rostral regions of the cortex are hypoactive, whereas the posterior regions of the cortex are hyperactive. Furthermore, the posterior inferior cerebellum is hyperactive in PSP. These new findings suggest that a distinct brain network across the basal ganglia, cortex, and cerebellum is uniquely impaired in PSP relative to PD.

Supplementary Material

Refer to Web version on PubMed Central for supplementary material.

Acknowledgments

This work was supported by the National Institutes of Health (R01 NS052318, R01 NS075012), National Parkinson Foundation Center of Excellence, Bachmann-Strauss Foundation, and the Wright/Fall/Simons Fund. MRI data collection was supported through the Human Imaging Core of the UF CTSI (UL1 TR000064) through the National Institutes of Health's Clinical and Translational Science Awards program, and the National High Magnetic Field Laboratory at the Advanced Magnetic Resonance Imaging and Spectroscopy.

Funding sources: National Institutes of Health (R01 NS052318, R01 NS075012), National Parkinson Foundation Center of Excellence, Bachmann-Strauss Foundation, and the Wright/Fall/Simons Fund. MRI data collection was supported through the Human Imaging Core of the UF CTSI (UL1 TR000064), the National Institutes of Health's Clinical and Translational Science Awards program, and the National High Magnetic Field Laboratory at the Advanced Magnetic Resonance Imaging and Spectroscopy.

References

1. Josephs KA, Dickson DW. Diagnostic accuracy of progressive supranuclear palsy in the Society for Progressive Supranuclear Palsy brain bank. Mov Disord. 2003; 18(9):1018–26. [PubMed: 14502669]
2. Williams DR, Lees AJ. Progressive supranuclear palsy: clinicopathological concepts and diagnostic challenges. Lancet Neurol. 2009; 8(3):270–9. [PubMed: 19233037]
3. Houghton DJ, Litvan I. Unraveling progressive supranuclear palsy: from the bedside back to the bench. Parkinsonism Relat Disord. 2007; 13(Suppl 3):S341–6. [PubMed: 18267262]
4. Litvan I, Agid Y, Calne D, Campbell G, Dubois B, Duvoisin RC, et al. Clinical research criteria for the diagnosis of progressive supranuclear palsy (Steele-Richardson-Olszewski syndrome) Report of the NINDS-SPSP International Workshop*. Neurology. 1996; 47(1):1–9. [PubMed: 8710059]
5. Ludolph AC, Kassubek J, Landwehrmeyer BG, Mandelkow E, Mandelkow EM, Burn DJ, et al. Tauopathies with parkinsonism: clinical spectrum, neuropathologic basis, biological markers, and treatment options. Eur J Neurol. 2009; 16(3):297–309. [PubMed: 19364361]
6. Brooks DJ. Diagnosis and Management of Atypical Parkinsonian Syndromes. J Neurol Neurosurg Psychiatry. 2002; 72(Suppl 1):i10–6. [PubMed: 11870198]
7. Zampieri C, Fabio RPD. Progressive Supranuclear Palsy: Disease Profile and Rehabilitation Strategies. Phys Ther. 2006; 86(6):870–80. [PubMed: 16737412]
8. Golbe LI. Progressive supranuclear palsy. Semin Neurol. 2014; 34(2):151–9. [PubMed: 24963674]
9. Spraker MB, Prodoehl J, Corcos DM, Comella CL, Vaillancourt DE. Basal ganglia hypoactivity during grip force in drug naïve Parkinson's disease. Hum Brain Mapp. 2010; 31(12):1928–41. [PubMed: 20225221]
10. Prodoehl J, Spraker M, Corcos D, Comella C, Vaillancourt D. Blood oxygenation level–dependent activation in basal ganglia nuclei relates to specific symptoms in de novo Parkinson's disease. Mov Disord. 2010; 25(13):2035–43. [PubMed: 20725915]
11. Prodoehl J, Planetta PJ, Kurani AS, Comella CL, Corcos DM, Vaillancourt DE. Differences in brain activation between tremor- and nontremor-dominant Parkinson disease. JAMA Neurol. 2013; 70(1):100–6. [PubMed: 23318516]

12. Neely KA, Kurani AS, Shukla P, Planetta PJ, Shukla AW, Goldman JG, et al. Functional Brain Activity Relates to 0–3 and 3–8 Hz Force Oscillations in Essential Tremor. Cereb Cortex. 2014:bhu142. [PubMed: 24962992]
13. Planetta PJ, Kurani AS, Shukla P, Prodoehl J, Corcos DM, Comella CL, et al. Distinct functional and macrostructural brain changes in Parkinson's disease and multiple system atrophy. Hum Brain Mapp. 2015; 36(3):1165–79. [PubMed: 25413603]
14. Yu H, Sternad D, Corcos DM, Vaillancourt DE. Role of Hyperactive Cerebellum and Motor Cortex in Parkinson's Disease. NeuroImage. 2007; 35(1):222–33. [PubMed: 17223579]
15. Wu T, Hallett M. The cerebellum in Parkinson's disease. Brain J Neurol. 2013; 136(3):696–709.
16. Tsuboi Y, Slowinski J, Josephs KA, Honer WG, Wszolek ZK, Dickson DW. Atrophy of superior cerebellar peduncle in progressive supranuclear palsy. Neurology. 2003; 60(11):1766–9. [PubMed: 12796528]
17. Kataoka H, Tonomura Y, Taoka T, Ueno S. Signal changes of superior cerebellar peduncle on fluid-attenuated inversion recovery in progressive supranuclear palsy. Parkinsonism Relat Disord. 2008; 14(1):63–5. [PubMed: 17481936]
18. Bloem BR, Hausdorff JM, Visser JE, Giladi N. Falls and freezing of gait in Parkinson's disease: a review of two interconnected, episodic phenomena. Mov Disord. 2004; 19(8):871–84. [PubMed: 15300651]
19. Williams DR, Watt HC, Lees AJ. Predictors of falls and fractures in bradykinetic rigid syndromes: a retrospective study. J Neurol Neurosurg Psychiatry. 2006; 77(4):468–73. [PubMed: 16543524]
20. Goetz CG, Tilley BC, Shaftman SR, Stebbins GT, Fahn S, Martinez-Martin P, et al. Movement Disorder Society-sponsored revision of the Unified Parkinson's Disease Rating Scale (MDS-UPDRS): scale presentation and clinimetric testing results. Mov Disord. 2008; 23(15):2129–70. [PubMed: 19025984]
21. Nasreddine ZS, Phillips NA, Bédirian V, Charbonneau S, Whitehead V, Collin I, et al. The Montreal Cognitive Assessment, MoCA: a brief screening tool for mild cognitive impairment. J Am Geriatr Soc. 2005; 53(4):695–9. [PubMed: 15817019]
22. Diedrichsen J. A spatially unbiased atlas template of the human cerebellum. NeuroImage. 2006; 33(1):127–38. [PubMed: 16904911]
23. Diedrichsen J, Balsters JH, Flavell J, Cussans E, Ramnani N. A probabilistic MR atlas of the human cerebellum. NeuroImage. 2009; 46(1):39–46. [PubMed: 19457380]
24. Mayka MA, Corcos DM, Leurgans SE, Vaillancourt DE. Three-dimensional locations and boundaries of motor and premotor cortices as defined by functional brain imaging: a meta-analysis. NeuroImage. 2006; 31(4):1453–74. [PubMed: 16571375]
25. Prodoehl J, Yu H, Little DM, Abraham I, Vaillancourt DE. Region of Interest Template for the Human Basal Ganglia: Comparing EPI and Standardized Space Approaches. NeuroImage. 2008; 39(3):956–65. [PubMed: 17988895]
26. Tzourio-Mazoyer N, Landeau B, Papathanassiou D, Crivello F, Etard O, Delcroix N, et al. Automated anatomical labeling of activations in SPM using a macroscopic anatomical parcellation of the MNI MRI single-subject brain. NeuroImage. 2002; 15(1):273–89. [PubMed: 11771995]
27. Noble JW, Eng JJ, Boyd LA. Effect of visual feedback on brain activation during motor tasks: an FMRI study. Motor Control. 2013; 17(3):298–312. [PubMed: 23761430]
28. Vaillancourt DE, Thulborn KR, Corcos DM. Neural basis for the processes that underlie visually guided and internally guided force control in humans. J Neurophysiol. 2003; 90(5):3330–40. [PubMed: 12840082]
29. Kuhtz-Buschbeck JP, Gilster R, Wolff S, Ulmer S, Siebner H, Jansen O. Brain activity is similar during precision and power gripping with light force: an fMRI study. NeuroImage. 2008; 40(4): 1469–81. [PubMed: 18316207]
30. Spraker MB, Corcos DM, Vaillancourt DE. Cortical and subcortical mechanisms for precisely controlled force generation and force relaxation. Cereb Cortex. 2009; 19(11):2640–50. [PubMed: 19254959]
31. Ehrsson HH, Fagergren A, Jonsson T, Westling G, Johansson RS, Forssberg H. Cortical activity in precision- versus power-grip tasks: an fMRI study. J Neurophysiol. 2000; 83(1):528–36. [PubMed: 10634893]

32. Brooks DJ, Ibanez V, Sawle GV, Quinn N, Lees AJ, Mathias CJ, et al. Differing patterns of striatal 18F-dopa uptake in Parkinson's disease, multiple system atrophy, and progressive supranuclear palsy. Ann Neurol. 1990; 28(4):547–55. [PubMed: 2132742]
33. Prodoehl J, Corcos DM, Vaillancourt DE. Basal Ganglia Mechanisms Underlying Precision Grip Force Control. Neurosci Biobehav Rev. 2009; 33(6):900–8. [PubMed: 19428499]
34. Vaillancourt DE, Yu H, Mayka MA, Corcos DM. Role of the basal ganglia and frontal cortex in selecting and producing internally guided force pulses. NeuroImage. 2007; 36(3):793–803. [PubMed: 17451971]
35. Bartels AL, de Jong BM, Giladi N, Schaafsma JD, Maguire RP, Veenma L, et al. Striatal dopa and glucose metabolism in PD patients with freezing of gait. Mov Disord. 2006; 21(9):1326–32. [PubMed: 16721756]
36. Macfarlane MD, Looi JCL, Walterfang M, Spulber G, Velakoulis D, Styner M, et al. Shape Abnormalities of the Caudate Nucleus Correlate with Poorer Gait and Balance: Results from a Subset of the LADIS Study. Am J Geriatr Psychiatry. 2015; 23(1):59–71. [PubMed: 23916546]
37. Robinson JL, Laird AR, Glahn DC, Blangero J, Sanghera MK, Pessoa L, et al. The functional connectivity of the human caudate: An application of meta-analytic connectivity modeling with behavioral filtering. Neuroimage. 2012; 60(1):117–29. [PubMed: 22197743]
38. Leh SE, Ptito A, Chakravarty MM, Strafella AP. Fronto-striatal connections in the human brain: a probabilistic diffusion tractography study. Neurosci Lett. 2007; 419(2):113–8. [PubMed: 17485168]
39. Buhmann C, Glauche V, Stürenburg HJ, Oechsner M, Weiller C, Büchel C. Pharmacologically modulated fMRI-cortical responsiveness to levodopa in drug-naive hemiparkinsonian patients. Brain. 2003; 126(2):451–61. [PubMed: 12538411]
40. Taniwaki T, Okayama A, Yoshiura T, Nakamura Y, Goto Y, Kira J, et al. Reappraisal of the motor role of basal ganglia: a functional magnetic resonance image study. J Neurosci. 2003; 23(8):3432–8. [PubMed: 12716951]
41. Alexander GE, Crutcher MD, DeLong MR. Basal ganglia-thalamocortical circuits: parallel substrates for motor, oculomotor, “prefrontal” and “limbic” functions. Prog Brain Res. 1990; 85:119–46. [PubMed: 2094891]
42. Keisker B, Hepp-Reymond MC, Blickenstorfer A, Meyer M, Kollias SS. Differential force scaling of fine-graded power grip force in the sensorimotor network. Hum Brain Mapp. 2009; 30(8):2453–65. [PubMed: 19172654]
43. Poon C, Coombes SA, Corcos DM, Christou EA, Vaillancourt DE. Transient shifts in frontal and parietal circuits scale with enhanced visual feedback and changes in force variability and error. J Neurophysiol. 2013; 109(8):2205–15. [PubMed: 23365186]
44. Singh-Curry V, Husain M. The functional role of the inferior parietal lobe in the dorsal and ventral stream dichotomy. Neuropsychologia. 2009; 47(6):1434–48. [PubMed: 19138694]
45. Ehrsson HH, Fagergren E, Forssberg H. Differential fronto-parietal activation depending on force used in a precision grip task: an fMRI study. J Neurophysiol. 2001; 85(6):2613–23. [PubMed: 11387405]
46. Grodd W, Hülsmann E, Lotze M, Wildgruber D, Erb M. Sensorimotor mapping of the human cerebellum: fMRI evidence of somatotopic organization. Hum Brain Mapp. 2001; 13(2):55–73. [PubMed: 11346886]
47. Mottolese C, Richard N, Harquel S, Szathmari A, Sirigu A, Desmurget M. Mapping motor representations in the human cerebellum. Brain J Neurol. 2013; 136(1):330–42.
48. Stoodley CJ, Schmahmann JD. Functional topography in the human cerebellum: a meta-analysis of neuroimaging studies. NeuroImage. 2009; 44(2):489–501. [PubMed: 18835452]
49. Kelly RM, Strick PL. Cerebellar loops with motor cortex and prefrontal cortex of a nonhuman primate. J Neurosci. 2003; 23(23):8432–44. [PubMed: 12968006]
50. Bernard JA, Seidler RD, Hassevoort KM, Benson BL, Welsh RC, Wiggins JL, et al. Resting state cortico-cerebellar functional connectivity networks: a comparison of anatomical and self-organizing map approaches. Front Neuroanat. 2012; 6:31. doi:10.3389/fnana.2012.00031.eCollection 2012. [PubMed: 22907994]

51. Buckner RL, Krienen FM, Castellanos A, Diaz JC, Yeo BTT. The organization of the human cerebellum estimated by intrinsic functional connectivity. J Neurophysiol. 2011; 106(5):2322–45. [PubMed: 21795627]
52. Vincent Prevosto WG. Cerebellar inputs to intraparietal cortex areas LIP and MIP: functional frameworks for adaptive control of eye movements, reaching, and arm/eye/head movement coordination. Cereb Cortex. 2009; 20(1):214–28. [PubMed: 19465740]
53. Glickstein M, Sultan F, Voogd J. Functional localization in the cerebellum. Cortex J Devoted Study Nerv Syst Behav. 2011; 47(1):59–80.
54. Shao N, Yang J, Li J, Shang HF. Voxelwise meta-analysis of gray matter anomalies in progressive supranuclear palsy and Parkinson's disease using anatomic likelihood estimation. Front Hum Neurosci. 2014; 8:63. [PubMed: 24600372]
55. Shi HC, Zhong JG, Pan PL, Xiao PR, Shen Y, Wu LJ, et al. Gray matter atrophy in progressive supranuclear palsy: meta-analysis of voxel-based morphometry studies. Neurol Sci. 2013; 34(7): 1049–55. [PubMed: 23543378]
56. Josephs KA, Whitwell JL, Eggers SD, Senjem ML, Jack CR Jr. Gray matter correlates of behavioral severity in progressive supranuclear palsy. Mov Disord. 2011; 26(3):493–8. [PubMed: 21462261]
57. Whitwell JL, Avula R, Master A, Vemuri P, Senjem ML, Jones DT, et al. Disrupted thalamocortical connectivity in PSP: a resting-state fMRI, DTI, and VBM study. Parkinsonism Relat Disord. 2011; 17(8):599–605. [PubMed: 21665514]
58. Kato N, Arai K, Hattori T. Study of the rostral midbrain atrophy in progressive supranuclear palsy. J Neurol Sci. 2003; 210(1-2):57–60. [PubMed: 12736089]
59. Paviour DC, Price SL, Jahanshahi M, Lees AJ, Fox NC. Regional brain volumes distinguish PSP, MSA-P, and PD: MRI-based clinico-radiological correlations. Mov Disord. 2006; 21(7):989–96. [PubMed: 16602104]
60. Righini A, Antonini A, De Notaris R, Bianchini E, Meucci N, Sacilotto G, et al. MR imaging of the superior profile of the midbrain: differential diagnosis between progressive supranuclear palsy and Parkinson disease. AJNR Am J Neuroradiol. 2004; 25(6):927–32. [PubMed: 15205125]
61. Dalaker TO, Zivadinov R, Larsen JP, Beyer MK, Cox JL, Alves G, et al. Gray matter correlations of cognition in incident Parkinson's disease. Mov Disord. 2010; 25(5):629–33. [PubMed: 20213820]
62. Rektorova I, Biundo R, Marecek R, Weis L, Aarsland D, Antonini A. Grey Matter Changes in Cognitively Impaired Parkinson's Disease Patients. PLoS ONE. 2014; 9(1):e85595. [PubMed: 24465612]
63. Summerfield C, Junqué C, Tolosa E, Salgado-Pineda P, Gómez-Ansón B, Martí MJ, et al. Structural brain changes in Parkinson disease with dementia: a voxel-based morphometry study. Arch Neurol. 2005; 62(2):281–5. [PubMed: 15710857]
64. Neely KA, Planetta PJ, Prodoehl J, Corcos DM, Comella CL, Goetz CG, et al. Force control deficits in individuals with Parkinson's disease, multiple systems atrophy, and progressive supranuclear palsy. PloS One. 2013; 8(3):e58403. [PubMed: 23505500]

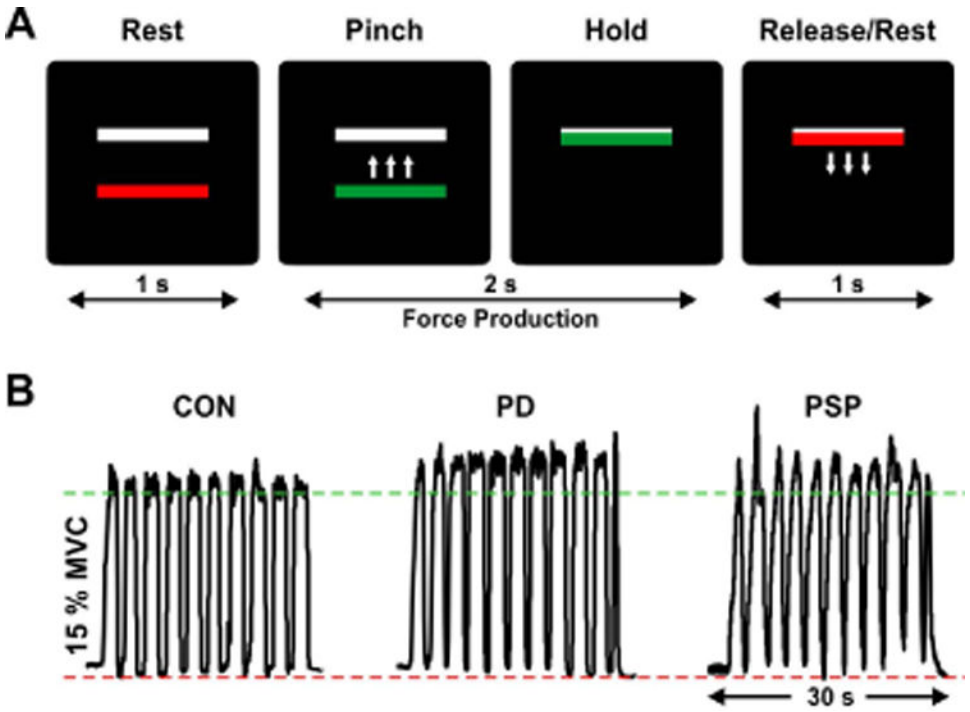

Fig. 1.

(A) Visual displays presented during the grip force task, in which participants were required to pinch the force transducer in order to move a colored bar on top of a stationary white bar and hold it there for 2 s. Green meant “go/force” and red meant “stop/no force”. Intertrial interval duration (rest period) was 1 s. Here, the feedback condition is shown, with visual feedback on the force produced (i.e. moving force bar). The no-feedback condition (not shown) lacked visual feedback on the moving force bar and consisted of memory-guided force generation. (B) Force traces of a representative healthy control (CON), Parkinson's disease (PD) patient, and progressive supranuclear palsy (PSP) patient for one block of the feedback condition. MVC, maximum voluntary contraction.

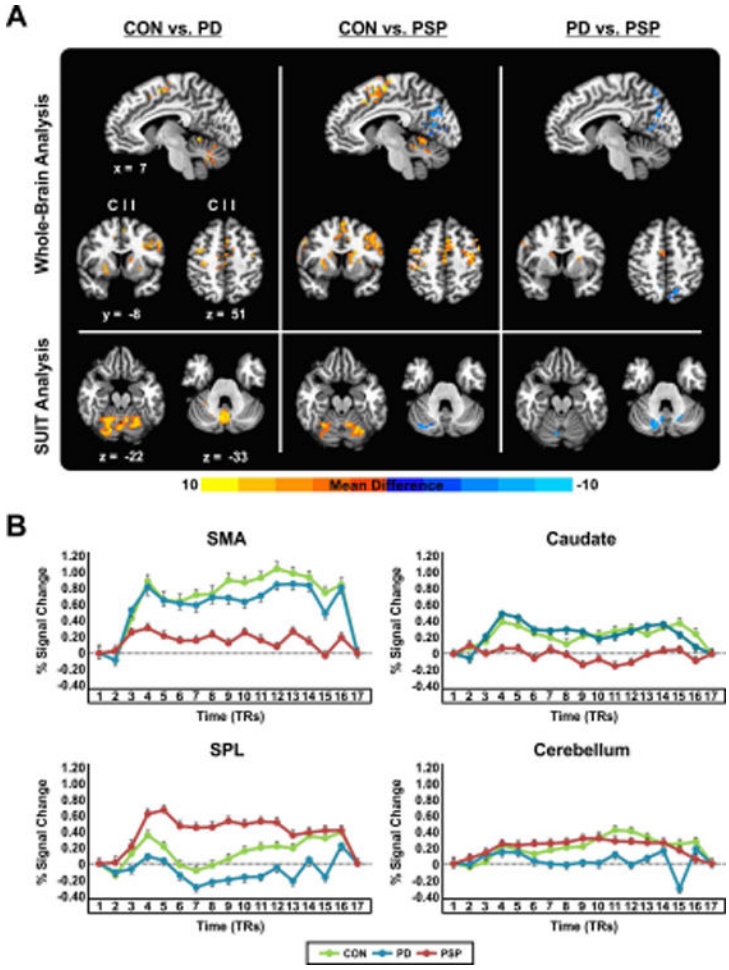

Fig. 2.

(A) Between-group force-related activation differences in the cortex (results of the whole-brain analysis) and cerebellum (results of SUIT analysis). Results are thresholded at $p < 0.005$ (cluster size correction using 3dClustSim in AFNI, providing a FWER corrected $p < 0.05$) and shown with respect to location in MNI space, and side. Positive values, represented by warm (red) colors indicate where BOLD activity was greater for controls compared to PD/PSP, and for PD compared to PSP. Negative values, represented by cool (blue) colors indicate where BOLD activity was greater for PSP compared to controls/PD. (B) Task-related percent signal change in the contralateral SMA, contralateral caudate, ipsilateral SPL, and posterior medial cerebellum, for controls, PD, and PSP. C, contralateral; CON, controls; I, ipsilateral; PD, Parkinson's disease; PSP, progressive supranuclear palsy; SMA, supplementary motor area; SPL, superior parietal lobule.

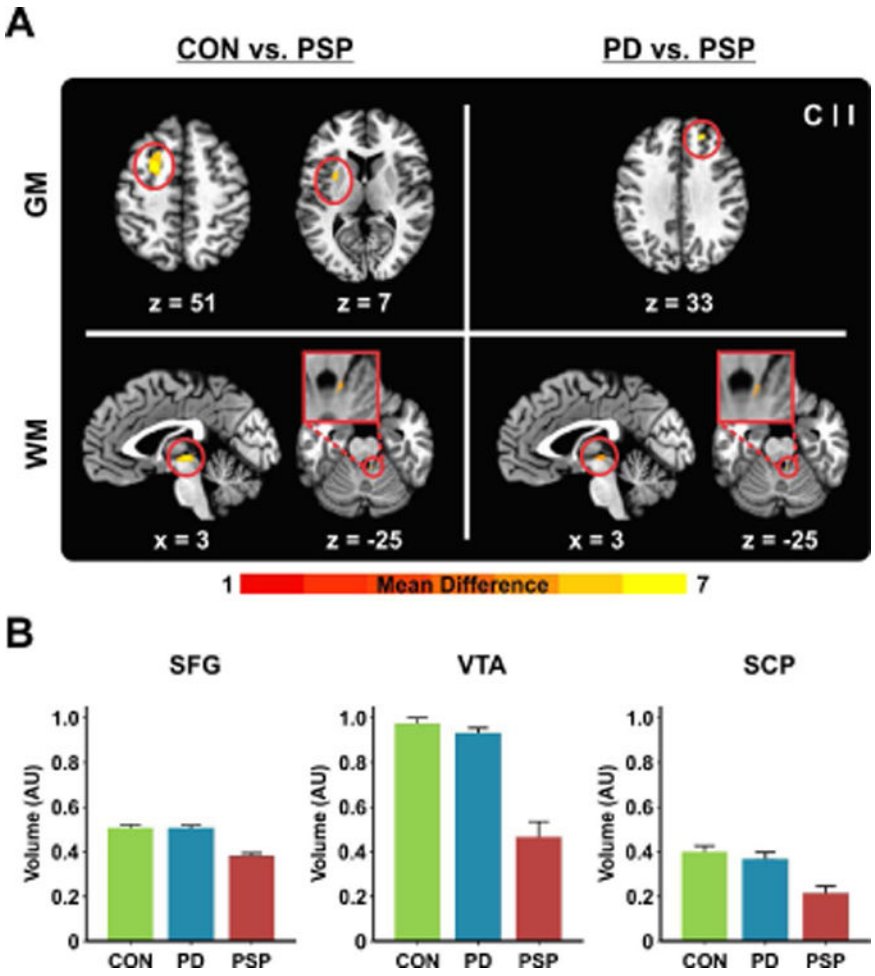

Fig. 3.

(A) VBM results showing between-group differences in regional GM/WM volume at a threshold of $p < 0.05$ (FWER corrected). Results are shown with respect to location in MNI space, and side. The color bar reflects *t*-values. (B) Volume of the ipsilateral superior frontal gyrus, ventral tegmental area, and ipsilateral superior cerebellar peduncle, ploted for controls, PD, and PSP. AU, arbitrary unit; C, contralateral; CON, controls; GM, gray matter; I, ipsilateral; PD, Parkinson's disease; PSP, progressive supranuclear palsy; SCP, superior cerebellar peduncle; SFG, superior frontal gyrus; VTA, ventral tegmental area; WM, white matter.

Table 1

Demographic and clinical characteristics

Demographics	**CON**	**PD**	**PSP**	***p* value [CON-PD-PSP]**	***p* value [PD-PSP]**
Gender (M:F)	10:10	12:8	10:10	0.765	-
Handedness (L:R)	3:17	5:15	1:19	0.208	-
Hand tested (L:R)	7:13	11:9	11:9	0.344	-
Age, years	64.8 (8.8)	65.8 (8.0)	67.8 (7.1)	0.367	-
MVC, N	72.8 (21.5)	68.1 (17.4)	59.6 (26.3)	0.182	-
Disease duration, m	-	49.7 (19.8)	30.6 (31.6)	-	-
Hoehn & Yahr	-	2.0 (0.3)	2.6 (0.9)	-	-
MDS-UPDRS-III – Total	2.1 (1.6)	31.9 (9.6)	39.0 (14.5)	< 0.001	0.176
MDS-UPDRS-III – Gait and Posture	0.05 (0.2)	2.1 (1.8)	6.0 (4.9)	< 0.001	0.001
MoCA – Total	27.2 (1.8)	25.6 (3.0)	20.0 (5.6)	< 0.001	0.001

Data reported are sums or means (±SD), and *p* values corresponding to group statistics. Handedness was self-reported. Abbreviations: CON, controls; F, females; L, left; m, months; M, males; MoCA, Montreal Cognitive Assessment; MDS-UPDRS-III, part III of the Movement Disorder Society Unified Parkinson's Disease Rating Scale; MVC, maximum voluntary contraction; N, Newtons; PD, Parkinson's disease; PSP, progressive supranuclear palsy; R, right.

Table 2

Between-group differences in cortical and cerebellar fMRI activation

Brain region(s)	Side	Size (mm^3)	MNI coord. (peak)			*F*-value
			x	y	z	
CON > PD						
PMv*, middle frontal gyrus	I	5535	57	12	33	18.81
SMA*, pre-SMA	C	2349	-2	-16	60	10.10
PMd*, M1	I	1755	27	-12	60	17.18
Putamen*, GPe, GPi	I	1512	33	-6	3	20.14
M1*, S1	C	1350	-36	-21	63	24.57
PMv*, PMd, M1, S1	I	783	51	-6	36	10.74
SMA	C	783	-2	-27	51	12.93
Putamen	C	675	-24	6	-9	17.60
Putamen*, caudate, GPe	C	621	-24	0	9	17.64
PMd	C	621	-42	-3	51	12.70
Caudate	I	513	15	9	9	11.62
Middle frontal gyrus	C	486	-45	21	39	14.04
M1*, S1	I	486	45	-15	63	17.26
Middle temporal gyrus	I	405	42	-60	9	22.81
Putamen	I	378	21	15	-9	24.47
Middle frontal gyrus	C	378	-36	54	27	9.44
Inferior frontal gyrus (pars tri)	C	351	-36	30	0	15.58
Cerebellum: VI, V, I-IV, Crus I	I	10632	23	-57	-22	13.29
Cerebellum: VI, V, I-IV, Crus I	C	7424	-23	-63	-24	29.14
Cerebellum: Vermis VI, Crus II, VIIb, VIIIa/b	C	3875	-1	-67	-21	14.54
CON > PSP						
M1*, S1, SMA, pre-SMA, PMd, PMv, middle frontal gyrus, middle cingulate cortex, supramarginal gyrus	C	29241	-36	-36	75	8.53
Caudate*, putamen, GPe,	I	4428	15	-3	15	9.20
Putamen*, caudate, GPe, GPi	C	3753	-24	6	-9	15.41

Brain region(s)	Side	Size (mm^3)	MNI coord. (peak)			*F*-value
			x	y	z	
Superior temporal gyrus*, supramarginal gyrus	C	2403	-69	-27	18	27.25
PMd*, PMv	C	1593	-45	-3	63	10.43
Middle frontal gyrus	I	729	30	51	39	10.19
Inferior temporal gyrus	C	594	-63	-57	-12	10.29
Superior temporal pole	I	567	54	21	-9	9.01
Inferior frontal gyrus (pars orb)	C	540	-42	39	30	15.36
PMv*, inferior frontal gyrus (pars tri)	C	513	-57	21	33	19.01
Inferior frontal gyrus (pars tri)	I	486	42	30	3	8.52
Middle temporal gyrus	I	405	42	-60	9	20.66
Thalamus	I	351	12	-12	9	13.94
Inferior frontal gyrus (pars tri), insula	C	351	-36	21	9	9.82
Caudate	C	351	-12	-3	18	22.27
Superior parietal lobule	C	351	-39	-54	66	13.29
PMv	C	324	-66	3	18	15.94
Cerebellum: V, VI, I-IV	I	7824	12	-56	-17	20.30
Cerebellum: VI, Crus I	C	1928	-32	-54	-23	14.47
PSP > CON						
Lingual gyrus*, calcarine gyrus	I	3132	9	-54	6	25.18
Cuneus *, calcarine gyrus, lingual gyrus	I	3105	9	-96	21	16.04
Lingual gyrus	C	1728	-1	-72	0	10.48
Cuneus	I	1647	9	-84	39	10.51
Precuneus*, calcarine gyrus	C	918	-15	-57	24	14.74
Fusiform gyrus	I	378	27	-69	-9	22.99
Precuneus*, middle cingulate cortex	C	351	-9	-48	36	18.99
Cerebellum: IX	I	856	10	-54	-39	27.72
Cerebellum: Crus I	C	376	-34	-80	-33	13.23
PD > PSP						
Superior temporal gyrus*, inferior parietal lobule, S1	C	1593	-69	-27	18	16.04

Brain region(s)	Side	Size (mm^3)	MNI coord. (peak)			*F*-value
			x	y	z	
Anterior cingulate cortex*, caudate	C	1431	-8	26	16	11.83
Middle temporal gyrus	I	756	66	-42	-4	9.09
PMv*, M1	C	702	-63	3	30	9.23
SMA	C	378	-1	-6	57	9.42
Putamen	I	351	27	3	12	17.85
PSP > PD						
Calcarine gyrus*, superior occipital gyrus, lingual gyrus	I	1404	3	-84	9	12.56
Middle cingulate cortex	C	594	-12	-15	39	11.53
Precuneus*, superior parietal lobule	I	567	6	-72	57	14.84
Lingual gyrus	C	513	-6	-69	3	15.59
Cuneus, lingual gyrus	C	513	-12	-90	27	11.48
Cuneus	I	405	3	-78	27	9.05
Precuneus	C	324	-2	-64	62	12.33
Cerebellum: Crus I, Crus II, VI, vermis VI and VIIIa/b, IX	C	4792	-19	-77	-29	19.08

The table describes fMRI results with respect to the anatomical location, side, cluster size, and intensity (*F*-value). Only brain regions surviving a height threshold of $p < 0.005$ (cluster size correction using 3dClustSim in AFNI, providing a FWER corrected $p < 0.05$) are listed. Coordinates in MNI space of the voxel of maximum intensity within each region are given. Region at peak coordinate is noted with an asterisk. C, contralateral; CON, controls; ; coord, coordinates; GPe, globus pallidus externus; GPi, globus pallidus internus; I, ipsilateral; M1, motor cortex; pars orb, pars orbitalis; pars tri, pars triangularis; PD, Parkinson's disease; PMd, dorsal premotor cortex, PMv, ventral premotor cortex; PSP, progressive supranuclear palsy; S1, sensorimotor cortex, pre-SMA, pre-supplementary motor area; SMA, supplementary motor area.